Intracellular potassium under osmotic stress determines the dielectrophoresis cross-over frequency of murine myeloma cells in the MHz range

Intracellular potassium under osmotic stress determines the dielectrophoresis cross-over frequency of murine myeloma cells in the MHz range.

Journal:	*ELECTROPHORESIS*
Manuscript ID	elps.201700433.R1
Wiley - Manuscript type:	Research Paper
Date Submitted by the Author:	n/a
Complete List of Authors:	Chung, Colin; The University of Edinburgh, Institute for Integrated Micro & Nanosystems Pethig, Ronald ; The University of Edinburgh, School of Engineering Smith, Stewart; The University of Edinburgh, Institute for Bioengineering Waterfall, Martin; The University of Edinburgh, School of Biological Sciences
Keywords:	Dielectrophoresis, Intracellular potassium, High frequency DEP cross-over, Murine myeloma cells, Osmotic stress

Research Paper

Intracellular potassium under osmotic stress determines the dielectrophoresis cross-over frequency of murine myeloma cells in the MHz range

Colin Chung[1*], Ronald Pethig[1], Stewart Smith[2], Martin Waterfall[3].

School of Engineering, [1]Institute for Integrated Micro & Nanosystems,

[2]Institute for Bioengineering, University of Edinburgh, Edinburgh, UK;

*Present address: Cirrus Logic International (UK) Ltd., Quartermile, Edinburgh.

[3]Institute of Immunology & Infection Research, School of Biological Sciences,

University of Edinburgh, Edinburgh, UK

Keywords:

Dielectrophoresis / Intracellular potassium / High frequency cross-over / Murine myeloma cells / Osmotic stress /

Communicating Author: Professor Ronald Pethig

Postal address (for galley proofs):

Lleyn,

Telford Road,

Menai Bridge

Anglesey LL59 5DT,

UK

Ron.Pethig@ed.ac.uk

Abstract:

Dielectrophoresis (DEP) has been widely studied for its potential as a biomarker-free method of sorting and characterizing cells based upon their dielectric properties. Most studies have employed voltage signals from ~1 kHz to no higher than ~30 MHz. Within this range a transition from negative to positive DEP can be observed at the cross-over frequency f_{x01}. The value of f_{x01} is determined by the conductivity of the suspending medium, as well as the size and shape of the cell and the dielectric properties (capacitance, conductivity) of its plasma membrane. In this work DEP measurements were performed up to 400 MHz, where the transition from positive to negative DEP can be observed at a higher cross-over frequency f_{x02}. SP2/O murine myeloma cells were suspended in buffer media of different osmolarities and measurements taken of cell volume, f_{x01} and f_{x02}. Potassium-binding benzofuran isophthalate (PBFI), a potassium-sensitive fluorophore, and flow cytometry was employed to monitor relative changes in intracellular potassium concentration. In agreement with theory, it was found that f_{x02} is independent of the cell parameters that control f_{x01} and is predominantly determined by intracellular conductivity. In particular, the value of f_{x02} is highly correlated to that of the intracellular potassium concentration.

1 Introduction

Under appropriate experimental conditions both theory [1-3] and experiment (*e.g.*, [4-5]) show that dielectrophoresis (DEP) of viable mammalian cells exhibits three modes of behaviour with increasing frequency of the applied electric field. At the so-called 'cross-over' frequency f_{xo1} a transition from negative to positive DEP occurs, whilst at the much higher frequency f_{xo2} there is a transition back to negative DEP [6,7]). At f_{xo1} and f_{xo2} the DEP force is zero, corresponding to the effective dielectric properties of the cell exactly matching those of the volume of suspending medium displaced by the cell. Because the value of f_{xo1} is sensitive to the shape of a cell, the dielectric properties of spherical, ellipsoidal and discoid cells can be evaluated if appropriate geometrical parameters are employed [8-10]. This paper describes investigations of the little explored characteristics of f_{xo2}, and to place this into context it is useful to summarise the current situation regarding f_{xo1}.

As reviewed elsewhere [10-14], theoretical and experimental evaluations of f_{xo1} have been extensive and exploited in practical applications of DEP, such as the manipulation, separation, and isolation of target cells from mixtures in suspension. Taking into account typical values for the size and dielectric properties of mammalian cells, f_{xo1} to a very good approximation is given by [15, 16]:

$$f_{xo1} = \frac{\sqrt{2}}{2\pi R C_m}\sigma_s - \frac{\sqrt{2}\,G_m}{8\pi C_m} \qquad (1)$$

In this equation R is the radius of a spherical cell, or the equivalent radius $(abc)^{1/3}$ of an ellipsoid with radii a, b, c, when suspended in a medium of conductivity σ_s. C_m and G_m are the capacitance and conductance of the cell membrane (per unit area).

Equation (1) is derived by applying the low-frequency DC approximations proposed by Schwan [17] for the effective conductivity ($\sigma_{eff} = RG_m$) and permittivity ($\varepsilon_{eff} = RC_m$) of a cell. Values for C_m can be obtained [16] from the slope of the plot of $f_{xo1}.R$ against σ_s, but accurate values for G_m derived from the intercept of such plots are only possible for restricted values of the frequency and medium conductivity [18]. The 2nd term on the right-hand side of Equation (1) is typically ~100-times smaller than the 1st term and is often neglected [11,19]. Determination of C_m can then be made from measurements of f_{xo1} and R at a known value for σ_s., but with the risk that the onset of passive ionic conductance due to degradation of the membrane's integrity will lead to significant underestimation of C_m.

Gascoyne *et al* [19] have summarised how C_m varies substantially between different cell types; cells in different states of differentiation; in different stages of the cell cycle; and following exposure of cells to apoptosis-inducing agents and toxicants. It was concluded that variations in C_m are related to membrane surface features such as ruffles, folds, and microvilli [20, 21], with the possibility that changes of membrane structure and chemistry should also be taken into account [22]. Whereas cell size does contribute significantly to dielectric differences between different cancer cell types, the value for C_m can also vary significantly among cells of the same size. Furthermore, under the same conditions, cancer cells exhibit consistently lower f_{xo1} values than peripheral blood cells [19]. These factors are of great significance regarding the development of DEP as a surface-marker independent and competitive technique for isolating circulating tumour cells from peripheral blood [23, 24].

Detailed experimental measurements of f_{xo2} for mammalian cells are, to our knowledge, restricted to an earlier report of our own for murine myeloma cells [25]. Values for f_{xo2} were observed in the region of 200 MHz, in agreement with theory based on known cell dielectric parameters. An unexpected finding was that f_{xo2} decreased steadily with time, in a temperature-activated (Arrhenius) manner. At 37°C, for example, f_{xo2} fell from ~200 MHz to ~80MHz after 2 hrs of suspension in the DEP medium. In this work we have extended our earlier study to clarify the factors influencing the value of f_{xo2}. We conclude that f_{xo2} is sensitive to the intracellular conductivity, a factor correlated to the osmotically induced alteration of internal potassium ion concentration. To achieve this result, the drift in f_{xo2} value was reduced to less than 10 MHz by performing the DEP measurements at 21°C and within 30 minutes of the cells being suspended in the DEP medium.

2 THEORY

A cells' DEP frequency response is defined by the Clausius-Mossotti factor [1-3]:

$$\frac{\varepsilon_c^* - \varepsilon_s^*}{\varepsilon_c^* + 2\varepsilon_s^*} \qquad (2)$$

The parameters ε_c^* and ε_s^* represent the complex permittivities of the cell and its suspending medium, which consist of electrically lossy dielectrics defined by:

$$\varepsilon^* = \varepsilon_0 \varepsilon - \frac{j\sigma}{\omega} \qquad (3)$$

where ε is the relative permittivity, ε_0 the permittivity of free space, σ the conductivity, ω the electric field angular frequency and j the imaginary vector, $\sqrt{-1}$. Equation (3) may be substituted directly into Equation (2) for the suspending medium,

which is effectively homogenous. A corresponding expression for the cell depends upon its heterogeneous structure and the frequencies under consideration. At sufficiently high frequencies, typically beyond 10 MHz and for a medium of 50 mS/m conductivity [10], the resistance of the plasma membrane is effectively short circuited by its capacitance, allowing the electric field to penetrate the cell interior. Understanding the behaviour of cells at these frequencies therefore requires a model incorporating their intracellular structure and dielectric properties. In the approach taken by Asami *et al* [26], a multi-shelled model built from concentric spheres was fitted to impedance measurements of mouse lymphocytes between 100 Hz and 250 MHz. Their model incorporated both the radii and complex permittivities of the cell membrane, cytoplasm, nuclear envelope and nucleoplasm. By substituting an effective expression for the complex permittivity of this structure into Equation (2) a nucleated cell's DEP frequency spectrum can be predicted [26]. An example for mouse lymphocytes is shown in Figure 1, modelled for three medium conductivities using the dielectric properties of the cell compartments derived by Asami *et al* [26]. In agreement with Equation (1) the value for f_{xo1} varies with changes in the medium conductivity σ_s, whereas f_{xo2} remains constant.

An analytical expression for f_{xo2} was first derived by Gimsa *et al* [6] and later simplified by Broche *et al* [27] to the following analytical expression:

$$f_{xo2} = \frac{\sigma_i}{2\pi\varepsilon_o}\sqrt{\frac{1}{2\varepsilon_s^2 - \varepsilon_i\varepsilon_s - \varepsilon_i^2}} \qquad (4)$$

where σ_i is the effective conductivity of the cell interior, and ε_o, ε_s, ε_i are the permittivity values of free space, the suspending medium and the cell interior, respectively. This formula may also be derived directly by assuming that the imposed

electric field frequency is significantly beyond that associated with Maxwell-Wagner interfacial polarisation of the plasma membrane. In this case the cell appears essentially as the cytoplasm with its internal contents [3]. This can be modelled as a multi-shelled dielectric sphere using the dielectric parameters for the cytoplasm and nucleus derived by Asami *et al* [26]. Equation (4) is then derived by assuming that the conductivity of the suspending medium is significantly below the intracellular value, a condition which can be satisfied experimentally. The proportionality of f_{xo2} with respect to intracellular conductivity, as indicated by Equation (4), breaks down in the limits of low intracellular and high medium conductivities [28]. For example, a deviation of 9% in the predicted value for f_{xo2} occurs when intracellular conductivity reduces by 50% in a 300 mS/m medium. However, with the suspending medium conductivity of 50 mS/m chosen for our experiments, the deviation from a direct 1:1 proportionality of f_{xo2} with the intracellular conductivity was no more than 1%. Finally, Equation (4) indicates that f_{xo2}, in sharp contrast with f_{xo1}, should be independent of cell radius R, membrane capacitance C_m, membrane conductance G_m, and the conductivity σ_s of the cell suspending medium.

Intracellular dielectric properties are difficult to measure in practice and typically require the fitting of multi-shelled dielectric models to impedance, electrorotation or DEP measurements across a range of frequencies. In this work we restricted ourselves to studying the changes in f_{xo2} as a function of intracellular potassium ion concentration $[K^+]_i$ - the most abundant intracellular ion [29]. Hypo-osmotic stress was used as a means of diluting the intracellular compartment, the reducing $[K^+]_i$, and with it the conductivity σ_i and, from Equation (4), the frequency f_{xo2}. Hypo-osmotic

stress was first explored by Kregenow [30] to induce the efflux of potassium from duck erythrocytes and later by Chimote [31] with human lens epithelial cells. We applied a similar stress by suspending cells in a medium nearly devoid of potassium, sodium or chloride ions and used mannitol to adjust osmolarity. Changes to $[K^+]_i$ were measured by ratiometric flow cytometry using a potassium sensitive fluorescent dye [32-34]. By measuring the volume of cells for a range of medium osmolalities we aimed to determine if a simple dilution model could account for the relative differences induced in both $[K^+]_i$ and f_{xo2}, and whether these quantities are indeed proportional to each other as we expect from Equation (4). In addition, measurements of f_{xo1} were made to provide information regarding the morphology and capacitance of the plasma membrane, in line with existing studies [15, 16, 19-22].

3 MATERIALS AND METHODS

All reagents were obtained from Life Technologies Corp. unless otherwise specified.

3.1 Cell Culture

The murine myeloma cell line SP2/O-AG14 was obtained from the American Type Culture Collection (Catalogue No. CRL1581). Cells were grown under standard tissue culture conditions as a suspension in RPMI-1640 supplemented with 10% Fetal Bovine Serum, 100 units/μg/ml penicillin-streptomycin (*i.e.*, 1:100 dilution of supplier's stock) and incubated at 37°C in a 5% humidified CO_2 atmosphere. The culture was maintained at a concentration typically between 0.25 and 1×10^6 cells/ml with regular feeding at 2 day intervals. In preparation for the experiments, 15 ml of SP2/O-AG14 cells were suspended at a density of 0.5×10^6 cells/ml and incubated overnight for 24 hours.

3.2 Potassium Sensitive Dye

The measurement of $[K^+]_i$ using the potassium-sensitive dye benzofuran isophthalate (PBFI) has been demonstrated with a variety of cell types [32-34]. The acetoxymethyl (AM) ester form of PBFI was dissolved in dimethyl sulfoxide (DMSO) at a stock concentration of 10 µM with 10 µl added to the culture media. To facilitate loading, 10 µl of Pluronic F-127 (20% w/v) was added and the cells incubated for 100 minutes. Extracellular PBFI was then removed by washing cells in fresh culture medium followed by an additional 60 minute incubation period. These loaded cells were suspended into phosphate buffered saline (PBS) and split for concurrent DEP and flow cytometry measurements. The cells were subsequently split and washed twice in 10 ml of DEP medium alongside a PBS control, with centrifugation between washes performed at 300g for 5 minutes.

3.3 DEP Cell-Suspending Media

Culture media contain a variety of components important for the long term maintenance and growth of cells. Typical formulations result in electrical conductivities of media exceeding 1 S/m. However, DEP measurements often require that the cells are suspended in a medium of conductivity less than 100 mS/m. This requirement demands the near complete removal of sodium and potassium chloride which constitute the main source of mobile, conducting ions. Our iso-osmotic (290 mOsm) formulation contained (in mM): 0.4 Ca^{2+}, 0.4 Mg^{2+}, 0.8 NO_3^- 0.4 SO_4^{2-}, 11 glucose, 10 HEPES and 267 mannitol. HEPES acted as a pH buffer in place of the standard sodium bicarbonate system used with CO_2, and the pH was adjusted to 7.4 using NaOH. Hypo-osmotic solutions were prepared at 140, 190, 215, and 240 mOsm by the removal of mannitol, with the resulting osmolarity measured using an

osmometer (Advanced Model 3300) and the conductivity determined as 42 mS/m using an Oakton CON-510 meter.

3.4 Determination of Intracellular K^+ and Membrane Integrity

A ratiometric measurement approach was used to determine relative internal potassium concentration, where the ratio of photoemissions at a characteristic wavelength is determined based on two distinct excitation wavelengths. This approach eliminates the impact of variations from both dye uptake and leakage. PBFI is relatively insensitive to changes in intracellular pH and intracellular sodium concentrations below 75 mM, exhibiting a fluorescent ratio with a near linear relationship to $[K^+]_i$ up to physiological levels [34]. Ratiometric measurements were performed on washed cells by flow cytometry (BD Biosciences LSR II). Excitation wavelengths of 355 and 405 nm were chosen which are close to the known excitation maxima and isobestic point of PBFI [32, 33]. Emissions were measured at ~500 nm and their ratio arising from excitations at both 355 and 405 nm were calculated. These ratios were normalised to that obtained for control samples suspended in PBS (~300 mOsm) and expressed as a percentage to provide a relative measurement of intracellular potassium concentration.

Cytometric analysis using the membrane impermeant fluorescent dye propidium iodide (PI) was employed to evaluate the proportion of apparently intact cells with damaged cytoplasmic membranes [35] in samples used for DEP analysis. As described in detail elsewhere [28] this technique provided information regarding the physical stability of cells suspended in DEP media of different osmolarity values.

3.5 DEP Cross-over (f_{xo1}, f_{xo2}) and Cell Diameter Measurements

The device used for DEP characterisation is described fully elsewhere [25, 28]. In brief, an array of sixteen 100 nm thick, 20 μm wide, platinum interdigitated electrodes spaced 40 μm apart were vacuum deposited onto a glass substrate. The final design, with a total effective capacitance of ~5 pF, was based on investigations to explore the impact of array size, electrode separation and solution conductivity on an applied electric signal. A circuit model based on a distributed RC network was evaluated and found to provide close agreement with practical impedance measurements. This was used to predict the voltage and phase along the electrode elements. A surface-mounted 50Ω resistor was connected in parallel with the electrode array, which was then soldered to a BNC connector to form a low pass filter. This arrangement provided a flat amplitude response below ~500 MHz, to ensure a constant field strength over the frequency range of interest, and was mounted into an inverted microscope (Meiji TC5100) equipped with a digital camera (Lumenera Infinity 2-3) for image capture.

Washed cells were suspended at a concentration of 1×10^7 cells/ml with 6.5 μl samples deposited onto the electrodes for analysis. A glass coverslip and gasket formed a chamber preventing any evaporation or disturbance of the sample. At the lower frequencies of f_{xo1} an Agilent 3324A signal generator supplied a 5V pk-pk sinusoid from 25 to 300 kHz. The frequency was increased in steps of 25 kHz lasting 5 seconds, which at the lower frequencies caused cells to levitate under negative DEP before attraction to the electrode edges by positive DEP above f_{xo1}. High frequency measurements of f_{xo2} used an Agilent ESD-4000A signal generator and a Mini-Circuits ZHL-1A amplifier generating a 4V pk-pk sinusoid. In a symmetrical manner

to f_{xo1} the frequency was swept downwards from 400 to 25 MHz in 5 seconds, 25 MHz steps, causing cells to initially levitate at high frequencies before being attracted to the electrode edges at frequencies lower than f_{xo2}. LabVIEW software controlled the camera and signal generators with images captured at each frequency step. By counting the cells that had been attracted, and then attached, by positive DEP to the edge of electrodes in these images the number within each band for f_{xo1} and f_{xo2} was determined. Cell diameter measurements were made by capturing images using a 40× objective. ImageJ software [36] was used to measure a sample of at least one hundred cells per datum using the various suspending media.

In previous work [25] we described how the value of f_{xo2} for cells suspended in DEP medium gradually decreased over time. The initial decrease of f_{xo2}, at 19 MHz/hr at 21 °C for the first two hours, limited the time that the cells could be suspended. In addition, the magnitude of the positive DEP force decreased steadily with time, leading to difficulties in clear observation of the attraction of cells to electrodes. The impact of this phenomenon was minimized by holding the PBFI-loaded cells in PBS prior to washing them into their respective DEP media, with the subsequent measurements performed within 30 minutes.

4 RESULTS AND DISCUSSION

Examples of forward (FSC) and side-scatter (SSC) plots are shown in Figure 2 for cells suspended in culture medium and the various DEP media. The trend observed of a reduction in FSC and an increase in SSC with increasing osmolarity is consistent with a reduction of cell size due to osmotic pressure, together with a corresponding

concentration increase of intracellular content. Also shown in this Figure is the percentage of intact cells in each sample, as determined by changes in the overall FSC and SSC heights compared to those obtained at nominal time zero for cells suspended in culture medium. In Figure 3 the FSC height versus PI fluorescence signal plots show the effect of increasing osmotic stress. The gated regions highlight intact cells with viable membranes, which when suspended in the original culture medium comprised 63.1% of the cell population. The corresponding intact and viable populations in the 270, 310 and 350 mOsm DEP media were 48.7%, 36.9% and 31.4%, respectively. As the osmolarity was reduced the median forward scatter increased towards that of the culture medium. The proportion of whole cells, relative to cell fragments, also increased. These distributions remained relatively constant up to four hours following initial cell suspension. These measurements and observations, described in more detail elsewhere [28], are consistent with the findings of Copp *et al* [37] that hyperosmotic stress induces apoptosis in mammalian cells, through inhibition of growth factor receptor signalling, induction of caspase-3 activation and reversible fragmentation of mitochondrial structure. Only those cells that appeared to be viable from their microscopic appearance (*e.g.*, typical size and no blebbing) were studied for their DEP response.

As shown in the inset of Figure 4, the volume of cells loaded with PBFI consistently decreased as the medium osmolarity was increased. Cells suspended in 215 mOsm DEP medium were found to have the same diameter, with similar relative forward and side scatter, as cells suspended in PBS of osmolarity ~300 mOsm. This was taken to indicate that for our mannitol-adjusted DEP media, the effective isotonic osmolarity was 215 mOsm. Higher osmolalities resulted in cell shrinkage with ~30% decrease in

volume at 290 mOsm (corresponding to a decrease from the isotonic value of 897±72 to 630±51 μm^3). This behaviour is similar to observations made by Rouzaire-Dubois *et al* [38] for murine glioma cells suspended into a medium in which half of the sodium chloride was substituted with sucrose. An observed 15% decrease in cell volume, which occurred within minutes, was attributed to the efflux of Na^+ and Cl^- due to their reduced extracellular concentrations. A study on human epithelial cells by Hamann *et al* [39] implicated the Na^+-K^+-2Cl^- cotransporter NKCC1 in facilitating this apparent isosmotic cell shrinkage under similar conditions. Our results suggest that by applying hypo-osmotic stress the original cell volume can be maintained at the effective isotonic osmolarity or increased further.

By plotting cell volume as a function of the inverse osmolarity, with both normalised to the isotonic osmolarity of 215 mOsm, a linear relationship of the Boyle-van't Hoff (BVH) form was found, as shown in Figure 4. The idealised BVH formula [40] is given by:

$$\frac{V_{BVH}}{V_{iso}} = (1 - v_b)\frac{M_{iso}}{M} + v_b \qquad (5)$$

where the modelled cell volume, V_{BVH}, and osmolarity, M, are normalised to the measured isotonic values of V_{iso} and M_{iso}. The osmotically inactive fraction of the cell volume v_b is represented by the intercept of this linear formula, which as shown in Figure 4 is close to zero.

As shown in Figure 5 the mean value of f_{xo1} decreased steadily with increasing osmolarity of the medium. After an initial increase in value with increasing osmolarity, f_{xo2} remained fairly constant over the hypertonic range of our experiments.

This is the range in which cell shrinkage was observed. As f_{xo2} is proportional to intracellular conductivity it should also depend on the concentration of mobile ions. The observed behaviour of f_{xo2} is therefore consistent with a net loss of ions from the intracellular compartment. By contrast, hypotonic stress resulted in f_{xo2} decreasing by 35%, from its isotonic value of 166±6 MHz to 108±4 MHz at 140 mOsm. Assuming the concentration of mobile intracellular ions remains constant, the BVH model for cell volume can be used to scale the isotonic value of $f_{xo2(iso)}$. This dilution factor, the isotonic volume V_{iso} divided by the modelled volume V_{BVH}, yields the following behaviour for f_{xo2}:

$$f_{x02(BVH)} = f_{x02(iso)} \times \frac{V_{iso}}{V_{BVH}} \quad (6)$$

where $f_{xo2(BVH)}$ is the predicted value of f_{xo2} based upon the fitted BVH model. In Figure 5 this is shown as the dashed line and fits the hypotonic data with an R^2 value of 0.929. At 140 mOsm a 36% volume increase corresponds to a 35% decrease in f_{xo2}. Under hypertonic conditions the model breaks down, overestimating f_{xo2} and suggests that if f_{xo2} is proportional to the intracellular concentration of mobile ions an efflux must be occurring. Based on this we can predict the proportion n of ions lost due to hypertonic stress as:

$$n = 1 - \frac{f_{xo2(hyper)} \times V_{hyper}}{f_{x02(iso)} \times V_{iso}} \quad (7)$$

where $f_{xo2(hyper)}$ and V_{hyper} are the hypertonic values for f_{xo2} and cell volume, respectively. Intracellular ion losses at 240 and 290 mOsm are estimated to be 18% and 29%, respectively. In the hypotonic region the value of n from Equation (7) remains close to zero.

DEP and ratiometric flow cytometry measurements were performed at the same time, in parallel, using the same cell suspension medium. The fluorescence ratio of the cells was calculated from their mean signal area intensity, and is plotted in Figure 6 as a percentage relative to that of a PBS suspended control. Between 140 mOsm and the isotonic value of 215 mOsm this ratio increased significantly, from 71±4% to 94±5%. Beyond this, the ratio increased only marginally to 99 ± 6% at 290 mOsm, which is a small change by comparison to the concomitant 30% decrease in cell volume. A physiological value for $[K^+]_i$ of 135 mM for our isotonic datum in DEP medium would imply an increase to 176 mM at 290 mOsm, assuming no efflux of ions. The fluorescent ratio is, however, known to behave in a non-linear manner at this concentration and to approach a maximum value, which could account for such a marginal increase in fluorescence [29]. By contrast, our observations of f_{xo2} strongly suggest that an efflux of intracellular ions is occurring. As there is no clear consensus between these two methods on the issue of hypertonic ion efflux, further study is necessary. Dezaki *et al* [41] have observed that HeLa cells placed under hypertonic stress observe an increase in $[K^+]_i$ and $[Cl^-]_i$ that is less than expected from the associated decrease in volume, suggesting that a net efflux of both ions under such conditions could indeed be occurring. As shown in Figure 7, a plot of f_{xo2} against the relative fluorescence ratio reveals a strong correlation between these two parameters. A straight line fit of the data gives an R^2 value of 0.967, which implies that f_{xo2} can provide an effective means of characterising cells based on their intracellular potassium concentration, particularly for those cells under isotonic or hypotonic conditions.

The variation of membrane capacitance C_{mem} with osmolarity is shown in Figure 8, and is consistent with previous studies [20]. The topographical changes involved can be expressed as a morphological factor ϕ, given as the ratio of C_{mem} over a theoretical value of 6 mF/m^2 for a typical smooth membrane [20]. At 140 mOsm, ϕ = 1.01, suggesting that our cells are extremely smooth and approaching the point of cytolysis. The isotonic point corresponds to ϕ = 1.66, increasing to ϕ = 2.41 at 290 mOsm. Broadly speaking, murine myeloma cells appear to behave as expected in terms of hypo-osmotic stress, f_{xo1} and cell volume.

5. Conclusions

This work has confirmed our earlier study [25] that measurement of the high-frequency DEP cross-over frequency f_{x02} for mammalian cells is practicable. An important conclusion is that f_{x02} is highly correlated to the intracellular conductivity, and in particular to its potassium concentration.

Measurements of cell volume, f_{xo1}, f_{xo2}, and intracellular potassium were made under varying degrees of osmotic stress. The cells closely obeyed the Boyle-van't Hoff ideal osmometer model. From measurements of both f_{xo1} and cell volume, the plasma capacitance was found to trend in a linear manner with osmolarity, approaching the expected value in the hypotonic extreme for a smooth lipid bilayer [20]. Over the observed hypertonic range f_{xo2} was found to be constant, indicating that an efflux of intracellular ions occurred, proportionate to the volume of water lost. Under increasing hypotonic stress the value of f_{xo2} decreased in a linear manner, consistent with a dilution of the intracellular ionic concentration resulting from the measured

increase in cell volume. Measurements using the potassium sensitive dye PBFI revealed that under increasing hypotonic stress the concentration of potassium also decreased in a linear manner, a relationship that strongly correlated to that of f_{xo2}.

Introduction of f_{xo2} as an investigative parameter can address new questions regarding the internal physico-chemical nature of cells, with the potential to further expand the analytical power of DEP. The critical role of potassium in many cell processes including volume regulation, growth and apoptosis, emphasise its importance as a biomarker. Our measurements of f_{xo2} suggest that DEP can be used to discriminate and sort cells based upon this. Although these initial studies reveal significant potential for exploitation, the extent to which intracellular ions, cell cycle and organelle structure affect f_{xo2} remain areas that merit further research.

We thank Drs Steve Pells, Vlastimil Srsen and David Wright for their practical assistance and helpful discussions. This work was supported by a Wolfson Microelectronics Scholarship awarded to C.C., and funding to RP from the Edinburgh Research Partnership in Engineering and Mathematics (ERPem).

The authors declare no conflict of interest

6. References

[1] Jones, T. B., *Electromechanics of Particles*, Cambridge University Press, New York 1995.

[2] Morgan, H., Green, N. G., *AC Electrokinetics: Colloids and Nanoparticles*, Research Studies Press, Baldock 2003.

[3] Pethig, R., *Dielectrophoresis: Theory, Methodology and Biological Applications*, John Wiley & Sons, Chichester 2017.

[4] Adams, T. N. G., Turner, P. A., Janorkar, A. V., Zhao, F., Minerick, A. R., *Biomicrofluidics* 2014, *8*, 054109.

[5] Faraghat, S. A., Hoettges, K. F., Steinbach, M. K., van der Veen, D. R., Brackenbury, W. J., Henslee, E. A., Labeed F. H., Hughes, M. P., *Proc. Natl. Acad. Sci. USA* 2017, *114*, 4591-4596.

[6] Gimsa, J., Marszalek, P., Loewe, U., Tsong, T. Y., *Biophys. J*. 1991, *60*, 749-760.

[7] Wang, X-B., Pethig, R., Jones, T. B., *J. Phys. D: Appl. Phys.* 1992, *25*, 905-912.

[8] Green, N. G., Jones, T. B., *J. Phys. D: Appl. Phys.* 2007, *40*, 78-85.

[9] Sebastián, J. L., Muňoz, S., Sancho, M., Álvarez, G., Miranda, J. M., *Phys. Med. Biol*. 2007, *52*, 6831-6847.

[10] Lei U., Lo, Y. J., *IET Nanobiotechnology* 2011, *5*, 86-106.

[11] Pethig, R., *Biomicrofluidics* 2010, *4*, 02281.

[12] Cetin, B., Li, D., *Electrophoresis* 2011, *32*, 2410-2427.

[13] Gagnon, Z. R., *Electrophoresis* 2011, *32*, 2466-2487.

[14] R. Martinez-Duarte, R., *Electrophoresis* 2012, *33*, 3110-3132.

[15] Huang, Y., Wang, X-B., Becker, F. F., Gascoyne, P. R. C., *Biochim. Biophys. Acta*, 1996, *1282*, 76-84.

[16] Pethig, R., Jakubek, L. M., Sanger, R. H., Heart, E., Corson, E. D., Smith, P. J. S., *IEE Proc. Nanobiotechnol*. 2005, *152***,** 189-193.

[17] Schwan, H. P., *Adv. Biol. Med. Phys*. 1957, *5,* 147-209.

[18] Lei, U., Sun, P-H., Pethig, R., *Biomicrofluidics* 2011, *5*, 044109.

[19] Gascoyne, P. R. C., Shim, S., Noshari, J., Becker, F. F., Stemke-Hale, K., *Electrophoresis* 2013, *34*, 1042-1050.

[20] Wang, X-B., Huang, Y., Gascoyne, P. R. C., Becker, F. F., Hölzel, R., Pethig, R., *Biochim. Biophys. Acta* 1994, *1193*, 330-344.

[21] Huang, Y., Wang, X-B., Gascoyne, P. R. C., Becker, F. F., *Biochim. Biophys. Acta* 1999, *1417*, 51-62.

[22] Muratore, M., Srsen, V., Waterfall, M., Downes, A., Pethig, R., *Biomicrofluidics* 2012, *6*, 034113.

[23] Gupta, V., Jafferji, I., Garza, M., Melnikova, V., Hasegawa, D., Pethig, R., Davis, D., *Biomicrofluidics* 2012, *6*, 024133.

[24] Shim, S., Stemke-Hale, K., Tsimberidou, A. M., Noshari, J., Anderson, T. E., Gascoyne, P. R. C., *Biomicrofluidics* 2013, *7*, 011808.

[25] Chung, C., Waterfall, M., Pells, S., Menachery, A., Smith, S., Pethig, R., *J. Electr. Bioimp.* 2011, *2*, 64-71.

[26] Asami, K., Takahashi, Y., Takashima, S., *Biochim. Biophys. Acta* 1989, *1010*, 49-66.

[27] Broche, L. M., Labeed, F. H., Hughes, M. P., *Phys. Med. Biol.* 2005**,** *50***,** 2267-2274.

[28] Chung, C., *Dielectrophoretic investigations of internal cell properties*, Ph.D thesis, School of Engineering, The University of Edinburgh, 2015. http://hdl.handle.net/1842/10044

[29] Yu, S. P., Canzoniero, L. M. T., Choi, D. W., *Curr. Opin. Cell Biol*. 2001, *13,* 405-411.

[30] Kregenow, F. M., *J. Gen. Physiol*. 1971, *58,* 372-395.

[31] Chimote, A. A., Adragna, N. C., Lauf, P. K., *J. Cell. Physio*. 2010, *223,* 110-122.

[32] Kasner, S. E., Ganz, M. B., *Am. J. Physiol.* 1992, *262,* F462-F467.

[33] Andersson, B., Janson, V., Behnam-Motlagh, P., Henriksson, R., Grankvist, K., *Toxicol. In Vitro* 2006, *20*, 986-994.

[34] Dallaporta, B., Hirsch, T., Susin, S. A., Zamzami, N., Larochette, N., Brenner, C., Marzo, I., Kroemer, G., *J. Immunol*.1998, *160,* 5605-5615.

[35] Vermes, I., Haanen, C., Steffens-Nakken, H., Reutelingsperger, C., *J. Immunol. Meth*. 1995, *184*, 39-51.

[36] Schneider, C. A., Rasband, W. S., Eliceiri, K. W., *Nat. Methods* 2012, *9*, 671-675.

[37] Copp, J., Wiley, S., Ward, M. W., van der Geer, P., *Cell Physiol*. 2005, *288,* C403-C415.

[38] Rouzaire-Dubois, B., Ouanounou, G., O'Regan, S., Dubois, J. M., *Eur. J. Physiol.* 2009, *457,* 1187-1198.

[39] Hamann, S., Herrera-Perez, J. J., Zeuthen, T., Alvarez-Leefmans, F. J., *J. Physiol*. 2010, *588,* 4089-4101.

[40] Katkov, I. I., *Cryobiology* 2011, *62*, 232-241.

[41] Dezaki, K., Maeno, E., Sato, K., Akita, T., Okada, Y., *Apoptosis* 2012, *17*, 821-831.

Figure Legends:

Figure 1. Modelled frequency dependence of the Clausius-Mossotti (CM) factor for mouse lymphocytes suspended in medium conductivities of 50, 200 and 300 mS/m, based on the dielectric data of Asami *et al* [26]. The DEP cross-over frequency f_{xo1} varies with the medium conductivity, whereas f_{xo2} remains constant.

Figure 2. Forward (FSC) and side-scatter (SSC) plots (25,000 event counts) obtained concurrently with DEP experiments for cells suspended in the (a) culture medium; (b)

270 mOsm medium; (c) 310 mOsm medium; (d) 350 mOsm medium. A clear trend is evident of a reduction in FSC and increase in SSC with increasing osmolarity. The number at the top-right of each plot gives the percentage of intact cells, as determined by changes in the overall FSC and SSC heights.

Figure 3. Plots of forward scatter height (FSC-H) versus propidium iodide uptake (FL2-H) by the cells. Each plot represents 25,000 cells in either (a) the culture medium, or DEP medium of osmolarity (b) 270 mOsm; (c) 310 mOsm; (d) 350 mOsm. The numbers given in the gated regions give an estimate of the proportion of cells with intact and impermeant membranes. Bands of signals from apoptotic bodies and cell fragments appear below the gated regions.

Figure 4. Boyle-van't Hoff plot for the murine myeloma cells, with the mean ± 95% confidence intervals shown (based on a spherical shape). The inset figure shows the variation of cell volume with osmolarity, where the isotonic volume was determined for cells suspended in PBS.

Figure 5. • Values of the cross-over frequency f_{x01} decrease with increasing osmolarity of the suspending medium, whereas f_{x02} (o data points) exhibits the opposite trend. The deviation above 215 mOsm of the experimental data points (o) for f_{x02} from that predicted by Equation (6) is discussed in the main text. All data points were obtained for a medium conductivity 41.5 mS/m. Error bars give ±95% confidence levels.

Figure 6. Flow cytometry analysis of PBFI fluorescence ratio, as a percentage of that obtained for the PBFI loaded control cells, in phosphate buffered saline solutions at different osmolarities. Error bars give ±95% confidence levels.

Figure 7. A linear relationship exists between values of the cross-over frequency f_{x02} and the PBFI fluorescence ratio determined from flow cytometry measurements. Error bars give ±95% confidence levels.

Figure 8. Dependence of membrane capacitance C_m with medium osmolarity, determined using Equation (1) from measurements of f_{xo1} and the mean cell diameter of 50 cells suspended at each osmolarity value for a medium conductivity of 41.5 mS/m. A negligibly small value was assumed for the membrane conductance G_m.

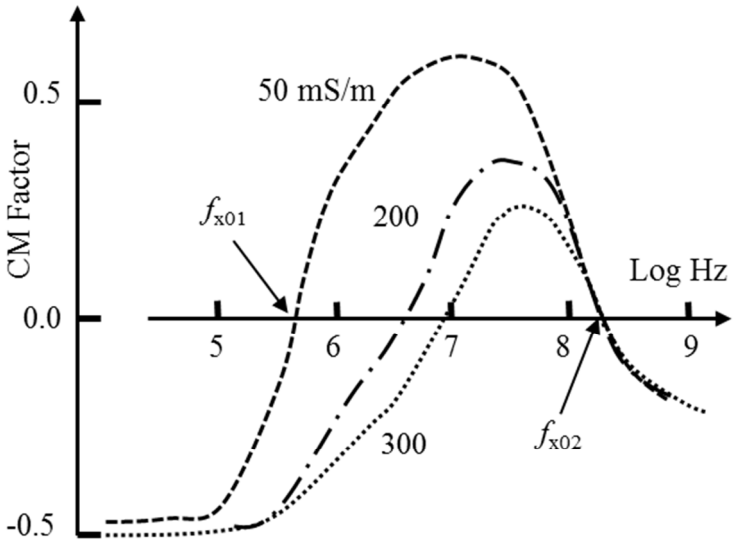

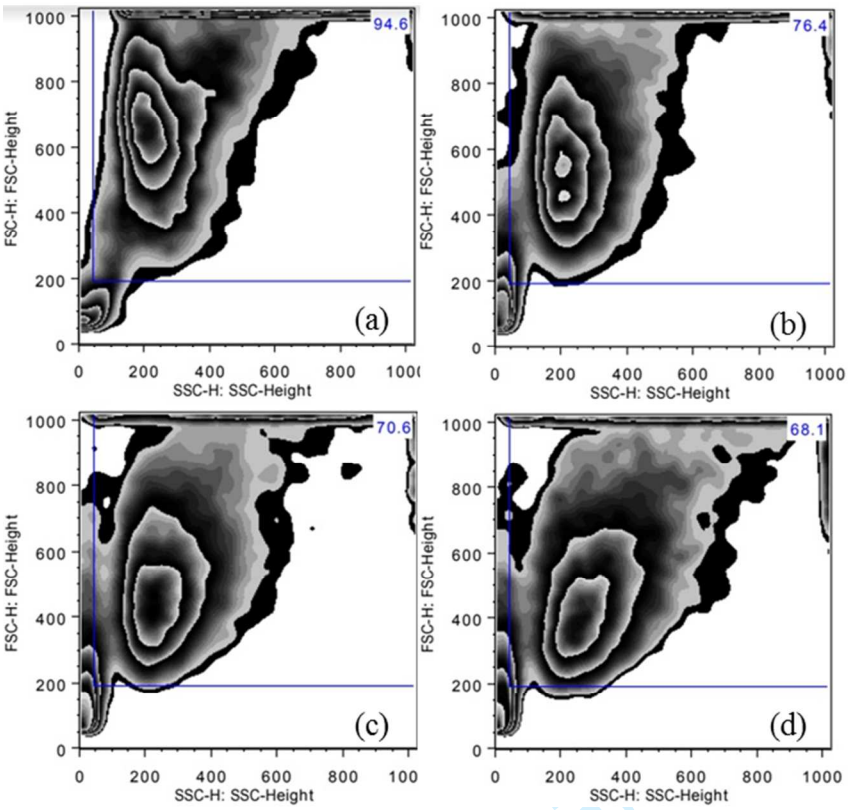
94.6
(a)
76.4
(b)
70.6
(c)
68.1
(d)
FSC-H: FSC-Height
SSC-H: SSC-Height
0
200
400
600
800
1000

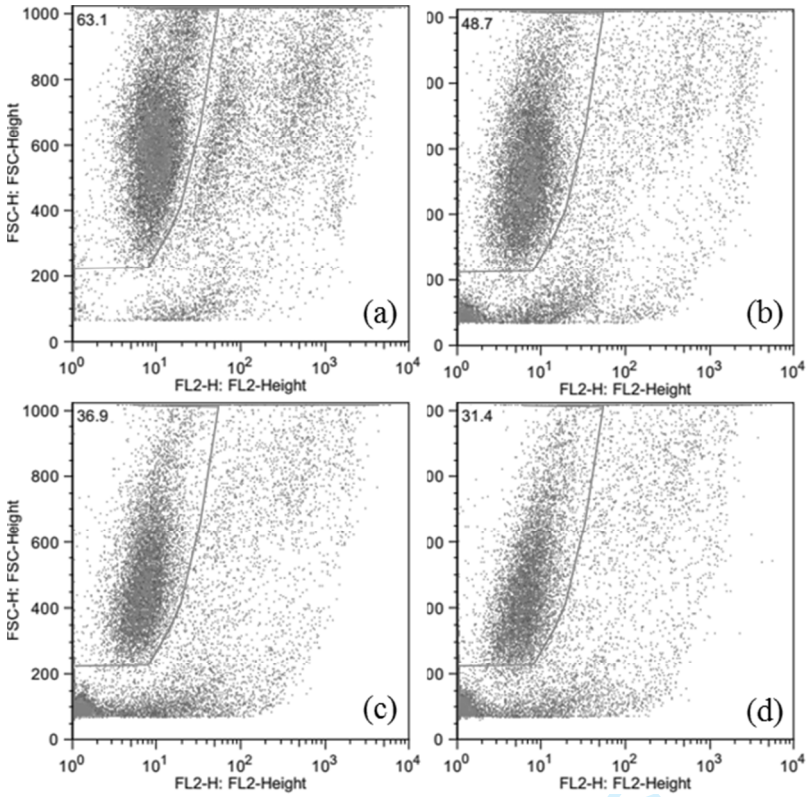
63.1
48.7
36.9
31.4
(a)
(b)
(c)
(d)
FSC-H: FSC-Height
FL2-H: FL2-Height
0
200
400
600
800
1000
10^0
10^1
10^2
10^3
10^4

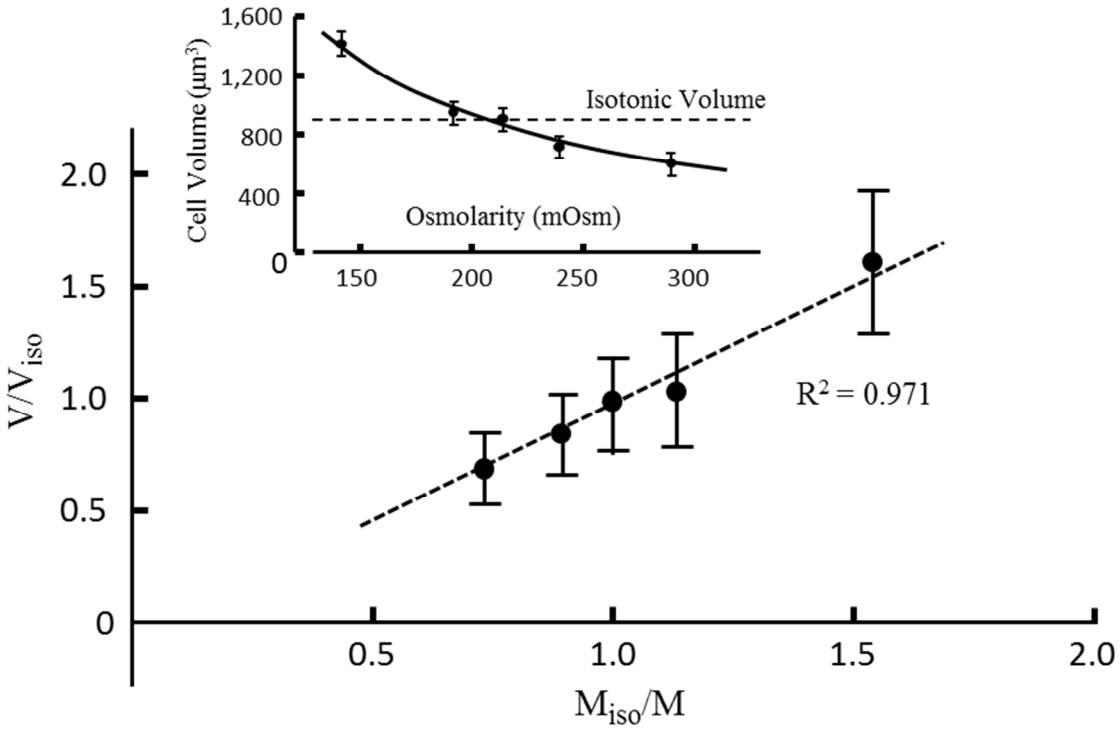
1,600
1,200
800
400
0
Cell Volume (μm³)
Isotonic Volume
Osmolarity (mOsm)
150
200
250
300
2.0
1.5
1.0
0.5
0
V/V_iso
R² = 0.971
0.5
1.0
1.5
2.0
M_iso/M

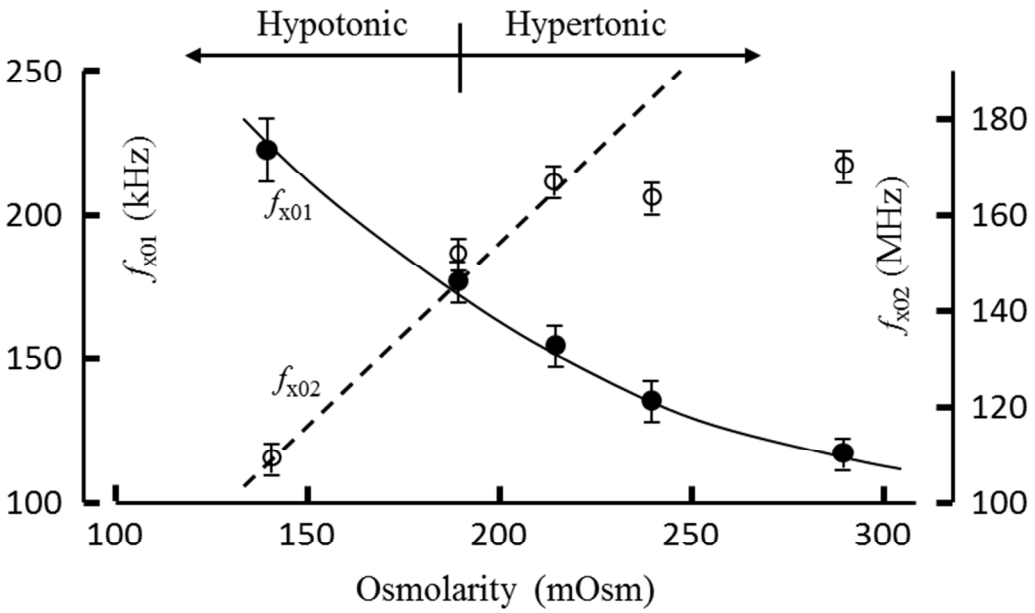
Hypotonic
Hypertonic
250
200
150
100
f_{x01} (kHz)
f_{x01}
f_{x02}
180
160
140
120
100
f_{x02} (MHz)
100
150
200
250
300
Osmolarity (mOsm)

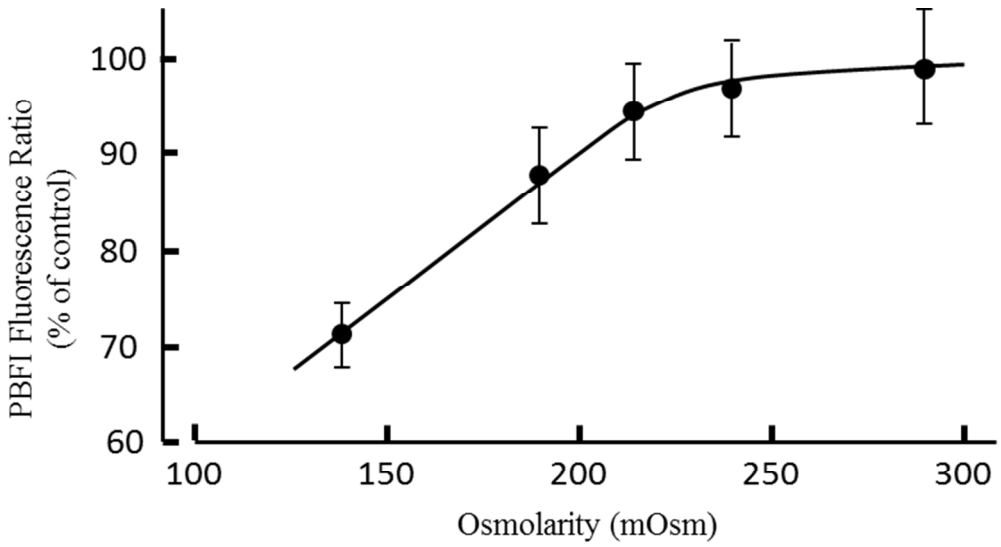
PBFI Fluorescence Ratio
(% of control)
100
90
80
70
60
100
150
200
250
300
Osmolarity (mOsm)

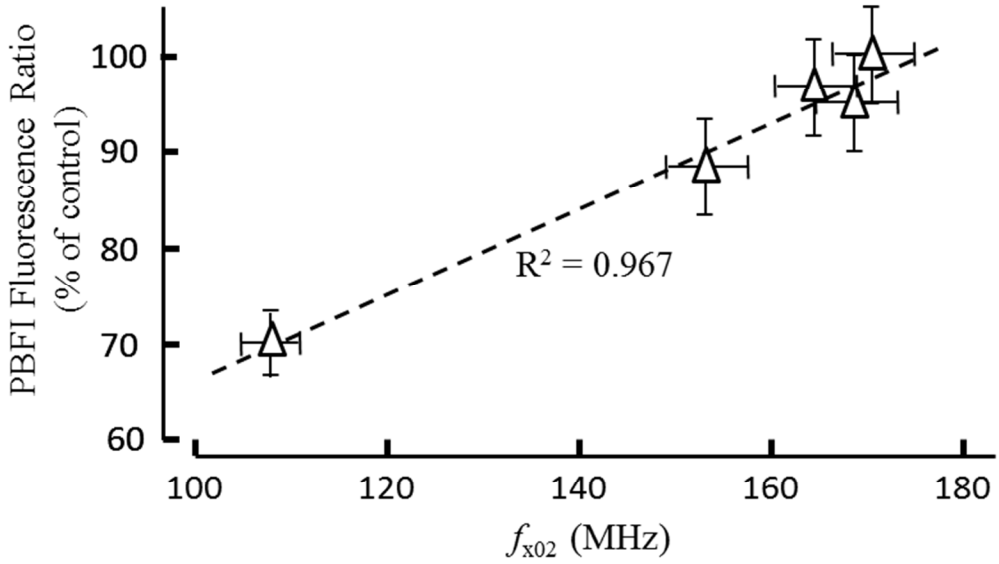
PBFI Fluorescence Ratio
(% of control)
100
90
80
70
60
100
120
140
160
180
f_{x02} (MHz)
$R^2 = 0.967$